

An investigation on characteristics of tracking failure in epoxy resin with harmonic and fractal dimension analysis

Mehmet Murat İSPİRLİ^{1,*}, Aysel ERSOY YILMAZ²

¹Department of Electrical and Electronics Engineering, Faculty of Technology, Marmara University, İstanbul, Turkey

²Department of Electrical and Electronics Engineering, Faculty of Engineering, İstanbul University, İstanbul, Turkey

Received: 04.05.2017

Accepted/Published Online: 14.11.2017

Final Version: 26.01.2018

Abstract: Epoxy resins have excellent mechanical and electrical properties; thus, they are commonly preferred in the electrical–electronic sector as insulation materials. These insulation materials experience degradation such as breakdown, tracking, or treeing. Therefore, safety and reliability tests of insulation materials have great importance in estimating the performance of insulation. These tests must be carried out to decrease the risk of electrical insulation fault. In this study, the relationship between tracking failures and the data obtained during experiments was evaluated. Tracking failure performance of epoxy resin was investigated using the IEC 60112 test standard, which is known as the comparative tracking index test. Leakage current data, collected from the experimental setup recorded from a ground electrode, were decomposed by using the Fourier transform method. The 3rd, 5th, and 7th harmonic distortion components of the leakage current data were calculated and their relationship with the number of drops falling on the sample was interpreted. Then the harmonic distortion components relationship was explained under dirty and clean surface conditions. We explained the tracking pattern formed on the surfaces of the samples after completion of the experiments was decomposed using image processing techniques. The capacity, information, and correlation dimensions of the resulting tracking patterns were calculated using fractal dimension analysis. Shapes in the same terms were examined using fractal dimension analysis.

Key words: Tracking failure, comparative tracking index, fractal dimension analysis, harmonic distortion component, tracking resistance

1. Introduction

Electrical insulation plays a vital role in the sustainability of electrical transmission systems and electrical devices. Failures in electrical insulation may result in the interruption of electrical transmission and the malfunction of electrical devices. Furthermore, failures in high-voltage insulation can cause severe problems.

Polymers are extensively used as electrical insulation materials due to their reliability, availability, ability to be easily processed, and low cost [1]. Several characteristics of polymers have been investigated to determine their long-term operational performance, such as tracking resistance, dielectric constant (ϵ), loss factor ($\tan \varphi$), and breakdown voltage. Tracking failure is defined as a dielectric breakdown occurring on the surface of polymers. Tracking resistance of an insulation material should be investigated to test the safety and reliability of electrical insulation [2]. The tracking process can be examined as follows [3]:

- A heat increase occurs on the surface due to electrical discharge. A tracking pattern is formed on the surface of a sample due to burning caused by this heat increase.

*Correspondence: mispirli@marmara.edu.tr

- Increased carbon density on the surface due to tracking pattern formations results in a greater heat increase.
- Finally, increased carbon density on the surface of a sample forms a conductive path, which leads to the breakdown of the sample [3].

Epoxy resins, when used in outdoor environments, are subject to environmental conditions that can form an ionized layer on the surface, such as moisture, dust, and salt. The International Electrotechnical Commission (IEC) 60112 test standard is used to model the environmental conditions to which insulation materials are subjected. This standard, also known as the comparative tracking index (CTI), gives fast, precise, significant, and comparative results about the durability and tracking resistance of the insulation material by simulating possible breakdowns that can occur on the surface of insulation materials [4].

Du et al. used two samples: unfilled (neat) polyethylene samples and polycarbonate samples filled with 3 wt.% polyethylene. They prepared 3-mm-thick samples of $20 \times 20 \times$ mm each from polymers and subjected them to gamma rays. Later, they investigated the behavior of gamma ray-saturated samples by using the tracking index test method. As a result of tests performed according to the IEC 60112 standard, the exposure of polycarbonate samples filled with 3 wt.% polyethylene to gamma rays increased their tracking resistance values. They observed that both erosion depth and weight loss values decreased when increasing the total dose from 0 to 100 kGy, whereas they increased when increasing the total dose from 100 to 1000 kGy for the modified polycarbonate sample. They determined the threshold value of tracking resistance for the modified polycarbonate as 100 kGy. Additionally, they indicated that the tracking resistance of unfilled polyethylene samples increased with an increasing dose of gamma rays. They concluded that exposure of polyethylene and modified polycarbonate samples to gamma rays increased their tracking resistances [4].

Chandrasekar investigated the tracking performances of samples prepared by adding 5, 10, 20, and 30 wt.% nano and micro aluminum oxide (Al_2O_3) particles to silicone rubber by using the CTI test method. Moreover, samples were subjected to accelerated aging tests for 30 days to determine the effects of environmental factors. For aging tests, samples were kept under ultraviolet light and immersed in an acid rain solution. As a result of tests performed by Chandrasekar in accordance with the IEC 60112 standard, it was determined that the reinforcement of silicone rubber with nano Al_2O_3 particles achieved better tracking resistances than that of micro Al_2O_3 particles. Considering weight loss in the samples, the author indicated that the tracking resistance values of the sample filled with 5 wt.% nano Al_2O_3 particles and the sample filled with 30 wt.% micro Al_2O_3 particles were similar at a rate of 3% [5].

The shapes of many structures in nature are complex and disordered. The use of fractal geometry is practical and useful for identifying such disordered structures. Studies using fractal geometry date back to nearly a hundred years. However, the acceleration of the development of fractal geometry has shown parallels to that of computer technology. Mandelbrot was the first scientist to carry out important studies of fractal geometry and obtained more significant results than any other scientist's work [6]. The development of computer technology has had an outstanding impact on this important progress. Fractal size analysis is suitable for use in many fields of science such as biology, chemistry, health, and spatial analysis. Shortly, it may be used in any field requiring analysis of a complex shape. In recent years, the fractal geometry concept has been used to evaluate tracking patterns formed on the surface of polymeric materials as a result of aging tests. Du et al. used it to analyze tracking patterns formed on the surfaces of cross-linked polyethylene (XLPE)-Si-rubber samples [7]. Kuntman et al. aged polyester samples according to the ASTM D2303 standard and analyzed tracking

patterns by using fractal geometry [8]. Similarly, Liu et al. analyzed microcracks and damage formed on the surface of SiR/SiO materials due to aging experiments by using fractal geometry [9].

In this study, the tracking performance of epoxy resin, widely used in the electrical-electronic sector for insulation, was investigated. A CTI experimental setup was established in the laboratory in accordance with the IEC 60112 test standard to determine tracking resistance. Before testing epoxy resin samples, their dielectric constant and loss factor values were measured at a utility frequency of 50 Hz in accordance with the IEC 60241 test standard. The relationship between the performance of the unfilled epoxy resin samples at 600 V and their tracking behavior was evaluated using fractal dimension analysis and harmonic distortion analyses of each vaporized drop.

2. Materials and methods

2.1. Comparative tracking index

An experimental setup to determine the CTI of epoxy resin was established based on the IEC 60112 test standard. The CTI test was first accepted by the International Electrotechnical Commission in 1959 [10]. In 2003, it was finalized in the IEC 112 standard. Later, it was developed by the ASTM and approved as D 5288 in 1992 [11]. Lastly, it was revised by the IEC and ASTM in 2009 and 2014, respectively [11,12]. The experimental setup, prepared in accordance with the IEC 60112 test standard, is shown in Figure 1.

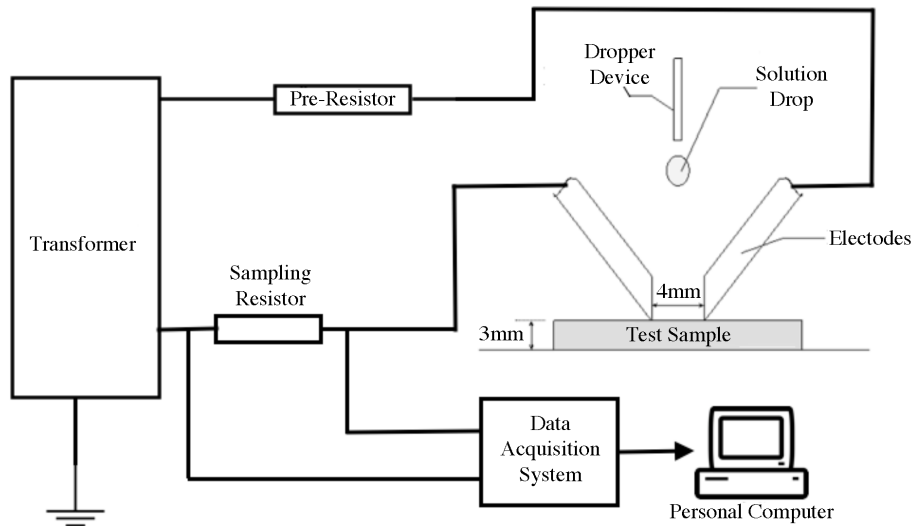


Figure 1. Schematic representation of the CTI experimental setup.

Copper electrodes of 5×2 mm, angled at 60° to each other, were used in this test. The minimum dimensions of the test insulation samples were $15 \times 15 \times 3$ mm and the force on the surface was 1 ± 0.05 N. The concentration of ammonium chloride (NH_4Cl) in the liquid to be dropped on the surface was $0.1 \pm 0.002\%$. Water used to prepare the solution should be deionized, and its resistivity at 23°C should be approximately $4 \Omega\text{m}$. The prepared solution is used in a setup to let a drop fall between the electrodes every 30 ± 5 s. The test is completed after 50 drops. According to the test standards, if a tracking pattern is observed before 50 drops have fallen onto the surface of a sample, or if the discharge current passing through the electrodes is above 0.5 A for at least 2 s, tracking failure has occurred [12–15].

The experimental setup was established in the High Voltage Techniques (HVT) Laboratory of İstanbul

University and was based on the IEC 60112 test standard, as shown in Figure 2. The electrode configuration used in the experimental setup is shown in Figure 3.

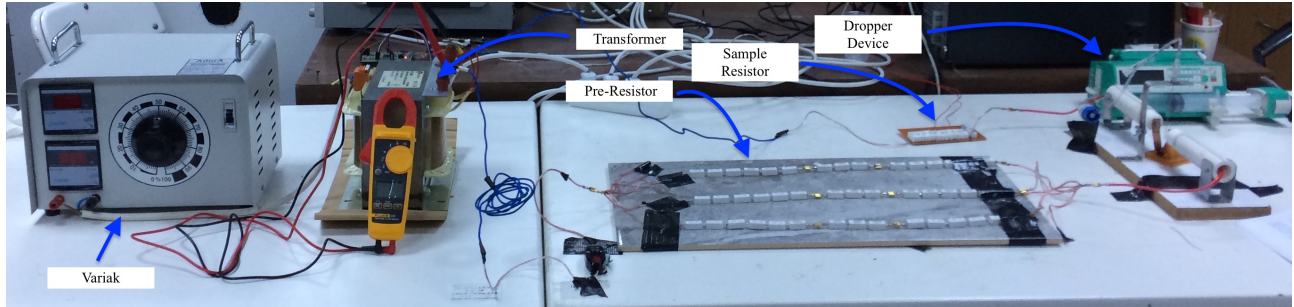


Figure 2. Experimental setup established in the HVT Laboratory.

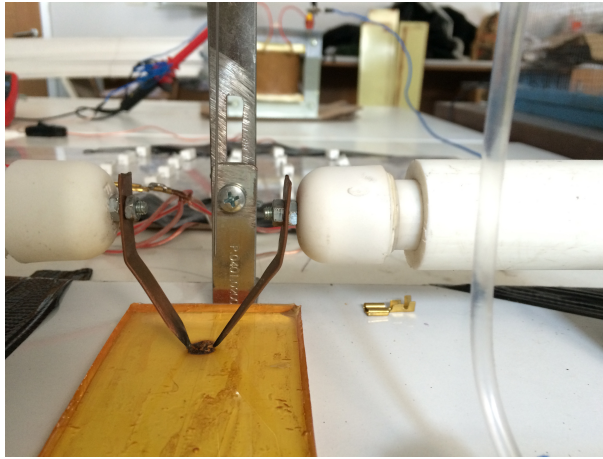


Figure 3. Electrode configuration used in the experimental setup.

The prepared epoxy resin samples obtained consist of two components: resin and hardener (mixture ratio: 2/1). Resin samples cured at 40 °C were molded to dimensions of 20 × 20 × 3 mm.

2.2. Harmonic analysis

Leakage current data were recorded from a ground electrode of the experimental setup during the CTI experiments carried out in this study. Recording was performed at 48,000 samples/s to clearly observe the breakdown via the leakage current data. These recorded data were decomposed into their harmonic components by computing Fourier transforms. Decomposition into harmonic components was calculated 5 s after the vaporization of each drop falling onto the sample surface. The reason for the choice of time interval was to observe high-amplitude discharge current, which starts at vaporization. The basic feature of a high-quality alternating current is a clean and smooth sinusoidal form. However, nonlinear components in systems cause corruptions in clean and smooth sinusoidal waves. Harmonic current components are constituted from nonlinear loads.

$$i(t) = \sum_{n=1}^{\infty} i_n(t) = \sum_{n=1}^{\infty} \sqrt{2} I_n \sin(n\omega_1 t + \delta_n)$$

Here, I_n and δ_n are the rms value of the current and the phase angle of the n_{th} harmonic, respectively. ω_1 is the angular frequency of the fundamental. In the equation, DC terms are ignored for simplicity. These corruptions are called harmonics. Harmonics can be at a frequency of 50, 150, 250, 350 Hz, etc. The fundamental (I_1) '50-Hz' component is called the fundamental or original harmonic component. The third harmonic component is the ratio of the 150-Hz component to the fundamental harmonic component, whereas the fifth harmonic component is the ratio of the 250-Hz component to the fundamental harmonic component. Similarly, the 7th, 9th, . . . , n th harmonic components are found by similarly dimensioning them to the fundamental harmonic component.

$$HD_n = \frac{I_n}{I_1}$$

Harmonics cause extra losses in engines, generators, capacitors, and energy transmission lines [16]. Ideal insulation materials are modeled as capacitance. Harmonic current components increase with increasing losses in capacitors, which leads to increased harmonics as well as insulation-induced losses. In this study, the 3rd, 5th, and 7th harmonic components of the leakage current data, recorded from the ground electrode of the experimental setup, were calculated using the Fourier transform method.

2.3. Fractal dimension analysis

Contrary to standard geometric shapes, tracking formed on the surface of insulation materials is disordered. These disordered structures cannot be evaluated by Euclidian geometry. Fractal geometry is used to evaluate such types of disordered structures. Complex geometric shapes showing self-resemblance features are called fractals. Fractals include tiny copies of themselves in their structures. In other words, they are geometric shapes repeating themselves at smaller scales. The most important feature of fractals is self-resemblance. This is very common in nature. Based on developments in computer technology, Mandelbrot was the first person who comprehensively investigated the fractal size analysis and obtained significant results [17]. Fractal size analysis originated as a study field in mathematics. However, nowadays it is used in various fields, such as biology, physical chemistry and fluid mechanics to analyze complex geometric shapes. In recent years, it has been used to analyze tracking formed on the surface of insulation materials as a result of accelerated aging methods using high voltage techniques [8,9,18–22].

Various approaches are used in calculating fractal dimensions: box-counting, fractal measure relations, correlation functions, and distribution functions. In this study, fractal dimensions of tracking occurring on the surface of samples were calculated by using the box-counting method. Mandelbrot presented the box number in L dimensions, $N(L)$, to be a power function as follows [17]:

$$N(L) = KL^{-D_x F},$$

where $N(L)$ is the number of boxes, K is a constant, L is the dimension, and DF is the fractal set of dimensions.

While evaluating tracking patterns occurring on the surfaces of epoxy samples by fractal dimension analysis, three quantifications in fractal dimension analysis were considered: the capacity dimension, the correlation dimension, and the information dimension.

The capacity dimension is used to calculate the fractal dimension of complex shapes [8,23,24]. Basically, the shape picture is divided into boxes, pixel by pixel. Frequency data are not considered in the calculation of the capacity dimension; rather, whether any box is empty or full is considered. In other words, the calculation depends on the logic response of the box (true or false). This dimension is called the capacity dimension because

it is calculated according to the data it includes. The capacity dimension in fractal dimension analysis is defined as follows:

$$D_{cap} = \frac{\ln N(\varepsilon)}{\ln(\frac{1}{\varepsilon})},$$

where $N(\varepsilon)$ is the number of boxes and ε is the side length of a box.

The correlation dimension is a fast and practical method to define the fractal dimension of a shape. It is defined in fractal dimension analysis as follows:

$$D_c = \frac{\sum_{i=1}^N P_i^2}{\ln \varepsilon},$$

$$P_i = \frac{n_i}{N},$$

where n_i is the number of points in the i th volume element and N is the total number of points in the trajectory.

The information dimension is a dimension value for the capacity dimension obtained by using probabilities. It can be defined as the point density in a certain cell. A fraction of the information is lost as the calculation of the capacity dimension approaches its mathematical limits. Lost information is referred to as the information dimension. The reason for the lost information is the complexity of its shape. The information and correlation dimensions are similar. The information dimension in fractal dimension analysis can be defined as follows:

$$D_i = \frac{\ln \sum_{i=1}^{N(\varepsilon)} P_i \ln P_i}{\ln \varepsilon},$$

$$P_i = \frac{n_i}{N},$$

where n_i is the number of points in the cell, N is the total number of points in the image, and $N(\varepsilon)$ is the minimum box size to cover the image.

3. Results

In this study, CTI tests were performed under laboratory conditions by using an experimental setup established in accordance with the IEC 60112 standard. A 600-V potential was applied to unfilled epoxy samples. All the samples used in this study were produced at the İstanbul University HVT Laboratory. Before testing the epoxy samples, their relative dielectric constant (ε_r) and loss factor ($\tan \varphi$) values were measured at a mains utility frequency of 50 Hz according to the IEC 60243-1 standards. IEC 60243-1:2013 provides test methods for the determination of the short-time electric strength of solid insulating materials at power frequencies between 48 and 62 Hz [25]. Therefore, the dielectric properties of all tested samples were verified. A 0.1% NH_4Cl solution was dropped onto the surface of the samples every 30 ± 5 s. The leakage current data passing through the sample surfaces were recorded for 50 drops, and the tracking pattern formed on the surface was observed after 50 drops. The 3rd, 5th, and 7th harmonic components were obtained from leakage current data by using a Fourier transform. The tracking pattern formed on the surface after 50 drops was evaluated in terms of fractal dimension.

The relative dielectric constant (ϵ_r) and loss factor ($\tan\varphi$) values at a mains utility frequency of 50 Hz for epoxy samples were measured according to IEC 60241 standards. By using those values, we calculated the capacitance and real and imaginary parts of the complex dielectric constant. The average obtained values for 5 samples are shown in Table 1.

Table 1. ϵ_r and $\tan\varphi$ values for prepared epoxy resins (*: measured value, **: calculated value).

Measurement frequency (Hz)	50 Hz
Capacitance (pF)**	82.57471714
Loss factor ($\tan\varphi$)*	0.044753057
Relative dielectric constant (ϵ_r)*	5.721763007
Real parts of the complex dielectric constant (ϵ')**	5.724653891
Imaginary parts of the complex dielectric constant (ϵ'')**	0.256195763

The changes in the 3rd, 5th, and 7th harmonic components of leakage current data, measured from the surface of the sample after ammonium chloride solution was dropped onto it, are shown in Figure 4. It is clearly seen that these harmonic components gradually increased until a tracking pattern failure was formed on the surface of the sample and then increased to a maximum after the 7th drop fell onto the surface of the sample, causing tracking failure. A decrease occurred in the magnitudes of the 3rd, 5th, and 7th harmonic components after the formation of a carbonized conductive path on the surface of the sample. For subsequent drops, these increases and decreases repeated themselves as a result of the tracking pattern, descending deeper into the surface. The most remarkable point was that the 5th harmonic component, measured just after the first drop, was higher than the 3rd harmonic component, whereas the 3rd harmonic component became higher than the 5th component as the impurity level increased on the surface of the sample after the first drop. Ahmedi-Joneidi et al. tested silicone rubber insulators according to the IEC 60507 standard. They indicated that the 5th harmonic component of insulators is higher than the 3rd harmonic component under clean conditions. However, under dirty conditions (i.e. high impurity levels), they indicated that the 3rd harmonic component was higher than the 5th harmonic component [26]. The findings obtained by Ahmedi-Joneidi et al. agree with those obtained in this study.

After repeated experiments were carried out at 600 V using 5 epoxy samples, a tracking pattern formed on the surfaces of 3 epoxy samples, which gave significant and consistent results. The tracking pattern was transformed into a monochrome image format using image processing methods. The capacity, information, and correlation fractal dimension values were calculated for the tracking produced. Uzunoğlu et al. evaluated the performance of tracking on the surface of polymeric materials, based on the IEC 587 inclined plane test standard. They used fractal geometry to investigate random tracking patterns formed on the surface of the samples. They indicated that the use of this method gives significant results when evaluating random tracking patterns [8]. A tracking pattern formed on the surface of the first epoxy sample and its capacity dimension graph is shown in Figure 5 while the calculated fractal dimension values of the first epoxy sample are shown in Table 2. The information and capacity dimension values take close values. The difference between the correlation dimension and these two dimension values is approximately 5%.

The tracking pattern formed on the surface of the second epoxy sample and its capacity dimension graph are shown in Figure 6, and the calculated fractal dimension values of the second epoxy sample are shown in Table 3. The difference between the capacity dimension values calculated in Figures 5 and 6 is approximately

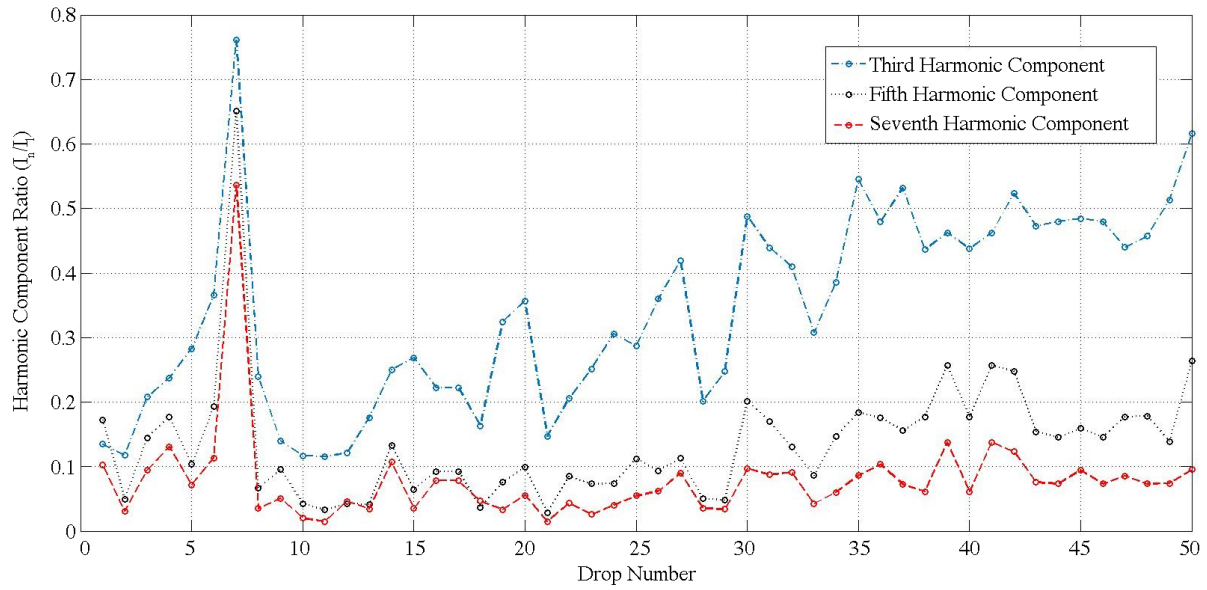


Figure 4. The 3rd, 5th, and 7th harmonic components of leakage current data for epoxy resins.

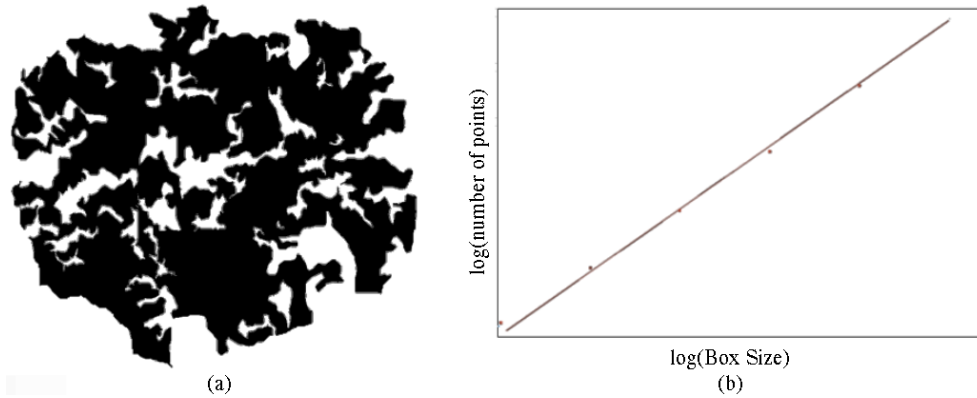


Figure 5. a) Tracking pattern formed on the surface of the first epoxy sample, b) capacity dimension graph.

Table 2. Fractal dimension values of the first epoxy sample.

Dimension calculated approach	Dimension value
Capacity dimension	1.79
Information dimension	1.78
Correlation dimension	1.89

3%, whereas the difference between the information dimension values is approximately 2.7%. However, the difference between the correlation dimension values is negligibly small.

The tracking pattern formed on the surface of the third epoxy sample and its capacity dimension graph is shown in Figure 7, and the calculated fractal dimension values of the third epoxy sample are shown in Table 4. The calculated capacity dimension values shown in Figures 6 and 7 are similar, whereas the difference between

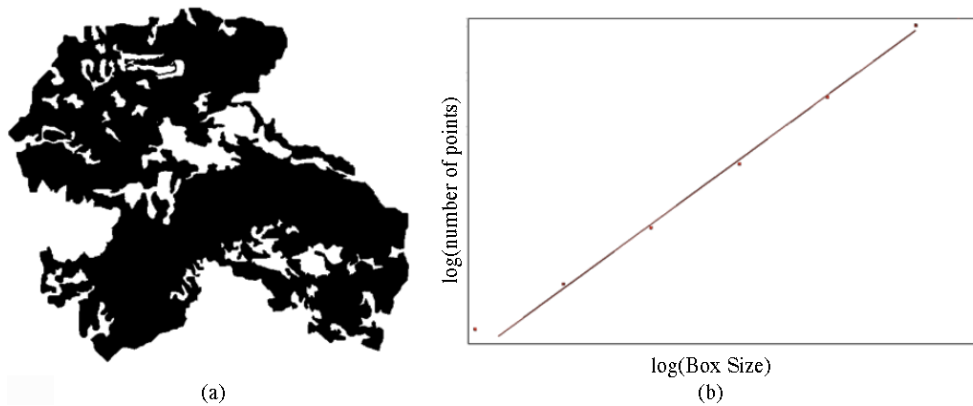


Figure 6. a) Tracking pattern formed on the surface of the second epoxy sample, b) capacity dimension graph.

Table 3. Fractal dimension values of the second epoxy sample.

Dimension calculated approach	Dimension value
Capacity dimension	1.73
Information dimension	1.83
Correlation dimension	1.892

the capacity dimension values calculated in Figures 5 and 7 is approximately 2.8%. On the other hand, the information dimension values calculated in Figures 6 and 7 are similar, whereas the difference between Figures 5 and 7 is 2.1%. Moreover, the difference between the correlation dimension value in Figure 5 and those in Figures 6 and 7 is approximately 5%.

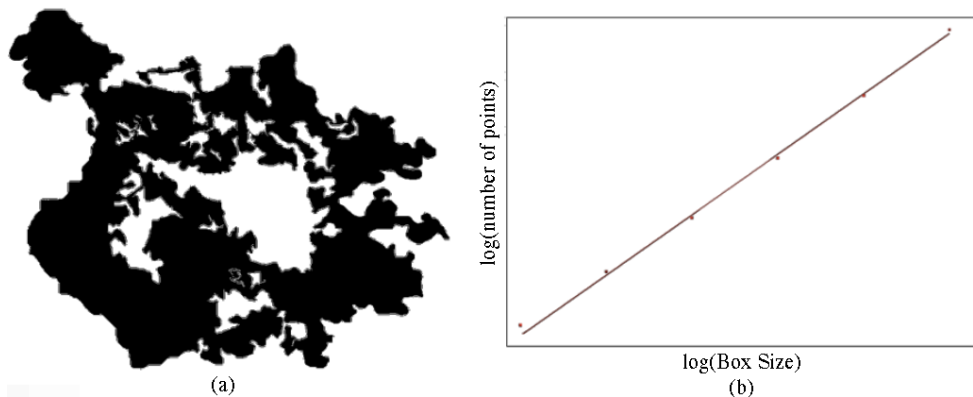


Figure 7. a) Tracking pattern formed on the surface of the third epoxy sample, b) capacity dimension graph.

The capacity, information, and correlation dimension values of three epoxy samples differed by a maximum of 1.83423%, 2.70304%, and 3.88815%, respectively. Therefore, although the tracking patterns formed on the surfaces of the samples are different, depending on the condition of the drop that falls, it can be said that the fractal dimension values of epoxy samples are consistent. Moon and Grassberger and Procaccia indicated that the difference between capacity, information, and correlation dimension values used in fractal dimension analysis were negligibly small [27,28]. Based on these studies, it can be deduced that there are small differences between

Table 4. Fractal dimension values of the third epoxy sample.

Dimension calculated approach	Dimension value
Capacity dimension	1.74
Information dimension	1.87
Correlation dimension	1.80

the values calculated using various equations. In this study, the difference between capacity, information, and correlation dimension values calculated for each tracking pattern is small, which reveals a parallel with the studies conducted by Moon and Grassberger and Procaccia.

4. Conclusion

This study was carried out to evaluate the performance of tracking pattern formation on the surface of epoxy resin material, which is used for electrical insulation. As a result of this study, the following observations were made:

- Tracking failure was observed after the 7th drop fell onto the surface of the epoxy resin sample.
- It was observed that the 3rd, 5th, and 7th harmonic distortion values reached their maxima at the 7th drop when tracking failure occurred. Additionally, as carbon density increased on the surface of the sample, these harmonic values decreased.
- Although the 5th harmonic distortion value calculated when the first drop fell onto the surface of the sample was higher than the 3rd harmonic distortion value, the 3rd harmonic distortion value was higher than the 5th harmonic distortion value for subsequent drops. The NH_4Cl solution used in this study models environmental impurity. Therefore, when the impurity level on the surface of a sample increases, it can be said that the 3rd harmonic distortion component starts to become higher than the 5th harmonic distortion component.
- The shape of the tracking pattern formed on the surface of the sample as a result of tests repeated at the same voltage level differed, depending on the condition of the drop falling onto it. These tracking patterns showed similar behaviors in terms of fractal geometry. According to this result, it is seen that evaluating the analysis of shapes with chaotic characteristics by using fractal geometry gives significant results.

Acknowledgment

This work was supported by the Scientific Research Projects Coordination Unit of İstanbul University (Project No. FBA-2016-22401).

References

- [1] Du B, Gao Y, Liu Y. Effects of gamma-ray irradiation on tracking failure of polymer insulating materials. In: Tsvetkov P, editor. *Nuclear Power: Operation, Safety and Environment*. Rijeka, Croatia: InTech, 2011. pp. 341-368.
- [2] Yoshimura N, Kumagai S, Du B. Research in Japan on the tracking phenomenon of electrical insulating materials. *IEEE Electr Insul M* 1997; 5: 8-19.

- [3] Ugur M. Modelling and analysis of surface tracking phenomena of solid insulating materials. PhD, University of Manchester, Manchester, UK, 1997.
- [4] Du B, Liu HJ. The application of recurrence plot in DC tracking test of gamma-ray irradiated polycarbonate. *IEEE T Dielect El In* 2009; 16: 17-23.
- [5] Chandrasekar S. Investigations on tracking and erosion resistance of nano silicone composite for high voltage outdoor insulation. *J Energ Power Eng* 2010; 4: 32-40.
- [6] Mandelbrot BB. *Fractals: Form, Chance and Dimension*. San Francisco, CA, USA: Freeman, 1977.
- [7] Du B, Zhu XH, Gu L, Liu HJ. Effect of surface smoothness on tracking mechanism in XLPE-Si-rubber interfaces. *IEEE T Dielect El In* 2011; 18: 176-181.
- [8] Kuntman A, Uğur M, Merev A. A study on the investigation of surface tracking in polyester insulators. In: EMO 1999 International Conference on Electrical and Electronics Engineering; 1-5 December 1999; Bursa, Turkey. Ankara, Turkey: EMO. pp. 84-88.
- [9] Liu Y, Zhang D, Xu H, Ale-Emran SM, Du B. Characteristic analysis of surface damage and bulk micro-cracks of SiR/SiO₂ nanocomposites caused by surface arc discharges. *IEEE T Dielect El In* 2016; 23: 2102-2109.
- [10] Mitchell GR. Present status of ASTM tracking test methods. *J Test Eval* 1974; 2: 23-31.
- [11] ASTM International. D5288-14. Standard Test Method for Determining Tracking Index of Electrical Insulating Materials Using Various Electrode Materials (Excluding Platinum). West Conshohocken, PA, USA: ASTM International, 2014.
- [12] IEC. Publication 60112. Method for the Determination of the Proof and the Comparative Tracking Indices of Solid Insulating Materials. 4th ed. Geneva, Switzerland: IEC, 2009.
- [13] IEC. Publication 112. Recommended Method for Determining the Comparative Tracking Index of Solid Insulating Materials under Moist Conditions. 2nd ed. Geneva, Switzerland: IEC, 1971.
- [14] IEC. Publication 112. Method for Determining the Comparative and the Proof Tracking Indices of Solid Insulating Material under Moist Conditions. 3rd ed. Geneva, Switzerland: IEC, 1979.
- [15] ASTM International. D3638-12. Standard Test Method for Comparative Tracking Index of Electrical Insulating Materials. West Conshohocken, PA, USA: ASTM International, 2012.
- [16] Esen V, Oral B, Akinci T. The determination of short circuits and grounding faults in electric power systems using time-frequency analysis. *J Energy South Afr* 2015; 26: 123-133.
- [17] Mandelbrot BB. On the geometry of homogeneous turbulence, with stress on the fractal dimension of the iso-surfaces of scalars. *J Fluid Mech* 1975; 72: 401-416.
- [18] Uzunoğlu CP, Uğur M, Kuntman A. Simulation of chaotic surface tracking on the polymeric insulators with Brownian motion. *İstanbul University, Journal of Electrical & Electronics Engineering*, 2008; 8: 585-592.
- [19] Kebbabı L, Beroual A. Fractal analysis of creeping discharge patterns propagating at solid/liquid interfaces: influence of the nature and geometry of solid insulators. *J Phys D Appl Phys* 2005; 39: 177-183.
- [20] Du B, Gu L. Effects of interfacial pressure on tracking failure between XLPE and silicon rubber. *IEEE T Dielect El In* 2010; 17: 1922-1930.
- [21] Du B, Zhang MM, Han T, Zhu LW. Effect of pulse frequency on tree characteristics in epoxy resin under low temperature. *IEEE T Dielect El In* 2016; 23: 104-112.
- [22] Ugur M, Varlow BR. Analyzing and modeling the 2D surface tracking patterns of polymeric insulation materials. *IEEE T Dielect El In* 1998; 5: 824-829.
- [23] Rasband SN. *Chaotic Dynamics of Nonlinear Systems*. Mineola, NY, USA: Dover Publications, 2015.
- [24] Moon FC. *Chaotic and Fractal Dynamics: An Introduction for Applied Scientists and Engineers*. Weinheim, Germany: Wiley, 2004.

- [25] IEC. 60243-1:2013. Electric Strength of Insulating Materials – Test Methods - Part 1: Tests at Power Frequencies. 3rd ed. Geneva, Switzerland: IEC, 2013.
- [26] [Ahmadi-Joneidi I, Majzooobi A, Shayegani-Akmal AA, Mohseni H, Jadidian J. Aging evaluation of silicone rubber insulators using leakage current and flashover voltage analysis. IEEE T Dielect El In 2013; 20: 212-220.](#)
- [27] Moon FC. Chaotic Vibrations: An Introduction for Applied Scientists and Engineers. New York, NY, USA: Wiley, 1987.
- [28] Grassberger P, Procaccia I. Measuring the strangeness of strange attractors. In: Hunt BR, Li TY, Kennedy JA, Nusse HE, editors. The Theory of Chaotic Attractors. New York, NY, USA: Springer, 2004.